Check for updates

Received: 27 July 2023 | Revised: 1 October 2023 | Accepted: 22 October 2023

DOI: 10.1111/cbdd.14415

RESEARCH ARTICLE

WILEY

Synthetic derivatives of natural cinnamic acids as potential anti-colorectal cancer agents

Federica Falbo[1] | **Sandra Gemma**[2] | **Adrian Koch**[3] | **Sarah Mazzotta**[4] | **Gabriele Carullo**[2] | **Anna Ramunno**[5] | **Stefania Butini**[2] | **Regine Schneider-Stock**[3] | **Giuseppe Campiani**[2] | **Francesca Aiello**[1]

[1]Dipartimento di Farmacia e Scienze della Salute e della Nutrizione, Università della Calabria, Rende, Cosenza, Italy

[2]Dipartimento di Biotecnologie, Chimica e Farmacia, Università degli Studi di Siena, Siena, Italy

[3]Experimental Tumorpathology, Institute of Pathology, Universitätsklinikum Erlangen, Friedrich-Alexander Universität Erlangen-Nürnberg, Erlangen, Germany

[4]Dipartimento di Chimica, Università degli Studi di Milano, Milano, Italy

[5]Dipartimento di Farmacia, Università degli Studi di Salerno, Fisciano, Salerno, Italy

Correspondence
Gabriele Carullo, Dipartimento di Biotecnologie, Chimica e Farmacia, Università degli Studi di Siena, Via Aldo Moro 2, Siena 53100, Italy.
Email: gabriele.carullo@unisi.it

Abstract

Cinnamic acid and its derivatives represent attractive building blocks for the development of pharmacological tools. A series of piperoniloyl and cinnamoyl-based amides (**6-9 a-f**) have been synthesized and assayed against a wide panel of colorectal cancer (CRC) cells, with the aim of finding promising anticancer agents. Among all twenty-four synthesized molecules, **7a**, **7e-f**, **9c**, and **9f** displayed the best antiproliferative activity. The induced G1 cell cycle arrest and the increase in apoptotic cell death was seen in FACS analysis and western Blotting in the colon tumor cell lines HCT116, SW480, LoVo, and HT29, but not in the nontumor cell line HCEC. In particular, **9f** overcame the resistance of HT29 cells, which have a mutant p53 and BRAF. Furthermore, **9f**, amide of piperonilic acid with the 3,4-dichlorobenzyl substituent upregulated p21, which is involved in cell cycle arrest as well as in apoptosis induction. Cinnamic acid derivatives might be potential anticancer compounds, useful for the development of promising anti-CRC agents.

KEYWORDS

amides, apoptosis, cell cycle, cinnamic acid, colorectal cancer, p21, piperonylic acid

1 | INTRODUCTION

Natural compounds display a plethora of amazing biological properties (Carullo et al., 2022; Pozzetti et al., 2022; Spizzirri et al., 2019). Among them, phenolic, hydroxycinnamic, and benzoic acids (general structure **1**, Figure 1) have been strongly investigated, and their role in both disease prevention and therapy has been extensively demonstrated (Carullo, Ahmed, et al., 2020; Carullo et al., 2021; Carullo, Governa, et al., 2019; Carullo, Perri, et al., 2019; Heleno et al., 2015; Mazzotta et al., 2021; Spizzirri et al., 2019). Phenolic and cinnamic acid derivatives are more efficient antioxidant agents than their benzoic analogs due to the resonance stabilization of the double bond, while relative to aromatic substitution, the antioxidant efficiency inside the class (benzoic or cinnamic) is *p*-hydroxydimethoxy >

Regine Schneider-Stock and Giuseppe Campiani—senior authors.

This is an open access article under the terms of the Creative Commons Attribution-NonCommercial-NoDerivs License, which permits use and distribution in any medium, provided the original work is properly cited, the use is non-commercial and no modifications or adaptations are made.
© 2023 The Authors. *Chemical Biology & Drug Design* published by John Wiley & Sons Ltd.

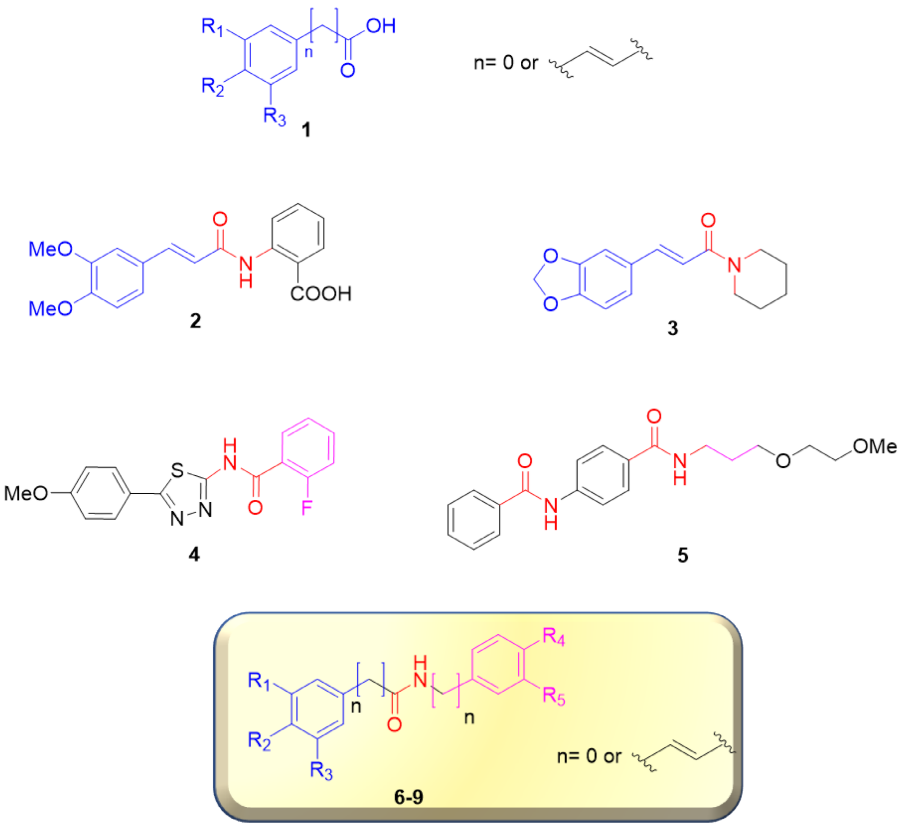

FIGURE 1 Design of new phenolic/cinnamic acid-based amides **6-9a-f**.

dihydroxy > *p*-hydroxymethoxy > *p*-hydroxy. Furthermore, the catechol moiety and the number of methoxy groups improve the antioxidant activity (Carullo et al., 2023), and sinapic acid is six times more efficient than Trolox® with respect to other benzoic acids (Natella et al., 1999).

In general, the key feature for the biological activity of these compounds is usually represented by the methoxy phenol moiety responsible for their antioxidant activity, anti-inflammatory activity, and antiproliferative activity (Nazir et al., 2020, 2022). 3,4,5-Trimethoxycinnamic acid esters and amide derivatives, which are widely distributed in natural products, are privileged structural scaffolds in drug discovery, and consequently, many chemical modifications have been carried out to improve drug-like properties and bioactive behavior (Zhao et al., 2019).

Pharmacological agents containing gallic acid in their structure exert different therapeutic activities, including antioxidant, anticancer, antimicrobial, chondroprotective, and antidiabetic activities, making this nucleus an attractive scaffold for the development of new pharmacological agents (Zahrani et al., 2020). Notably, many phenolic compounds are non-nucleoside inhibitors, leading to apoptosis of cancer cells and interfering with chromatin structure and functions (Federico et al., 2022; Hazafa et al., 2022). Furthermore, other phenolic/cinnamic derivatives interfere with the expression of different genes, often overexpressed in colorectal cancer (CRC) (Garmpis et al., 2021; Lee et al., 2022; Relitti et al., 2020; Saraswati et al., 2020).

However, cinnamic acid and its derivatives are usually used in fragrance materials, food, and cosmetics, with limited use as drugs, essentially due to their poor absorption. Among these compounds, only tranilast (**2**, Figure 1) and ilepcimide (**3**, Figure 1) demonstrated interesting antifungal, antimicrobial and antioxidant activities (Darakhshan & Pour, 2015; Kobzar et al., 2023; Vaishnav et al., 2023; Xu et al., 2023). For this reason, it could be profitable to design and synthesize hybrids of these compounds to obtain promising pharmacological tools. In this work, twenty-four differently decorated cinnamoyl derivatives were synthesized by combining piperonilic, sinapic, *trans*-cinnamic, and *trans*-3,4-(methylenedioxy)cinnamic acids with different primary amines to obtain amide derivatives.

Amide connection was used in these new structures considering that this functional group is one of the most recurrent in bioactive molecules (Ertl et al., 2020). Different anticancer compounds present amide functions in their structures as compound **4**; of note, this functional group is also an essential moiety interacting with metals, as exemplified by compound **5** (Sirous et al., 2021).

17470285, 2024, 1, Downloaded from https://onlinelibrary.wiley.com/doi/10.1111/cbdd.14415 by CochraneItalia, Wiley Online Library on [17/01/2024]. See the Terms and Conditions (https://onlinelibrary.wiley.com/terms-and-conditions) on Wiley Online Library for rules of use; OA articles are governed by the applicable Creative Commons License

All the synthesized amides (**6-9 a-f**) were initially assayed in HCT116 CRC cells to investigate their antiproliferative activity. Cell cycle was analyzed for the most interesting compounds to ascertain the cell death mechanism, suggesting p53/p21-mediated apoptosis. The positive modulation of p21 was hypothesized to be associated with increased levels of acetyl histone H3, although not significantly. These data were further confirmed in other CRC cells, such as LoVo, SW480, HT29, and DLD1 cells.

2 | RESULTS AND DISCUSSION

2.1 | Chemistry

The synthesis of compounds **6a**-**f**, **7a**-**f**, and **8a**-**f** is depicted in Scheme 1. The amides were synthesized starting from the corresponding carboxylic acids **10**–**12** by using 1-ethyl-3-(3-dimethylaminopropyl)carbodiimide (EDCI), 1-hydroxybenzotriazole (HOBt) and the appropriate amine as reported by Ghosh and Shahabi (2021). *trans*-Cinnamic acid **10** was reacted with benzylamine to obtain **6a**, 4-fluorobenzylamine for **6b**, 4-chlorobenzylamine for **6c**, 4-chlorophenethylamine for **6d**, 4-fluorophenethylamine for **6e**, and 3,4-dichlorobenzylamine to obtain **6f**. *trans* 3,4-(Methylenedioxy)cinnamic acid **11** was used to synthesize **7a**-**f** using suitable amines under the same experimental conditions. Finally, sinapic acid **12** was employed for the synthesis of amides **8a**-**f** (Scheme 1). The amides **9a**-**f** were synthesized starting from piperonilic acid **13** (Scheme 2), transformed into its acyl chloride (not isolated), and then treated with different amines under Schotten–Baumann conditions.

2.2 | Biological experiments

2.2.1 | Crystal violet assay revealed high cytotoxicity for compounds **7a**, **7e**, **7f**, **9c**, and **9f**

We started with a screening experiment, examining the antiproliferative properties of the single compounds using HCT116 colon cancer cells (Figure 2). In the first set of experiments, compounds **6a**-**f**, **7a**-**f**, **8a**-**f**, and **9a**-**f** were tested at concentrations of 0.1, 1, 10, 50, and 100 μM. Compounds **6a**-**f**, a series of cinnamic amides, did not show interesting

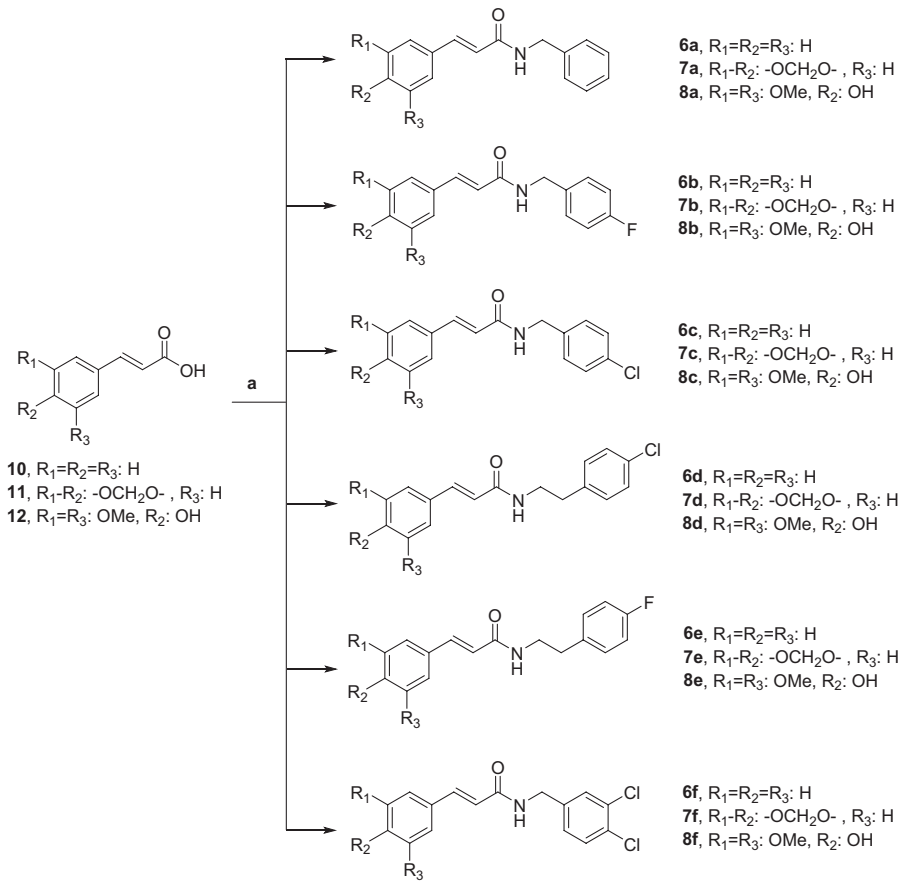

SCHEME 1 Synthesis of compounds **6a**-**f**, **7a**-**f**, **8a**-**f**. For compounds **6a**-**f**, *trans*-cinnamic acid (1.00 eq.), for compounds **7a**-**f**, *trans* 3,4-(methylenedioxy)cinnamic acid (1.00 eq.), for compounds **8a**-**f**, sinapic acid (1.00 eq.), appropriate amine (1.20 eq.), EDCI (2.10 eq.), HOBt (1.5 eq.), dry DMF (10 mL), 25°C, 24 h. EDCI, 1-ethyl-3-(3-dimethylaminopropyl)carbodiimide; HOBt, 1-hydroxybenzotriazole.

17470285, 2024, 1, Downloaded from https://onlinelibrary.wiley.com/doi/10.1111/cbdd.14415 by CochraneItalia, Wiley Online Library on [17/01/2024]. See the Terms and Conditions (https://onlinelibrary.wiley.com/terms-and-conditions) on Wiley Online Library for rules of use; OA articles are governed by the applicable Creative Commons License

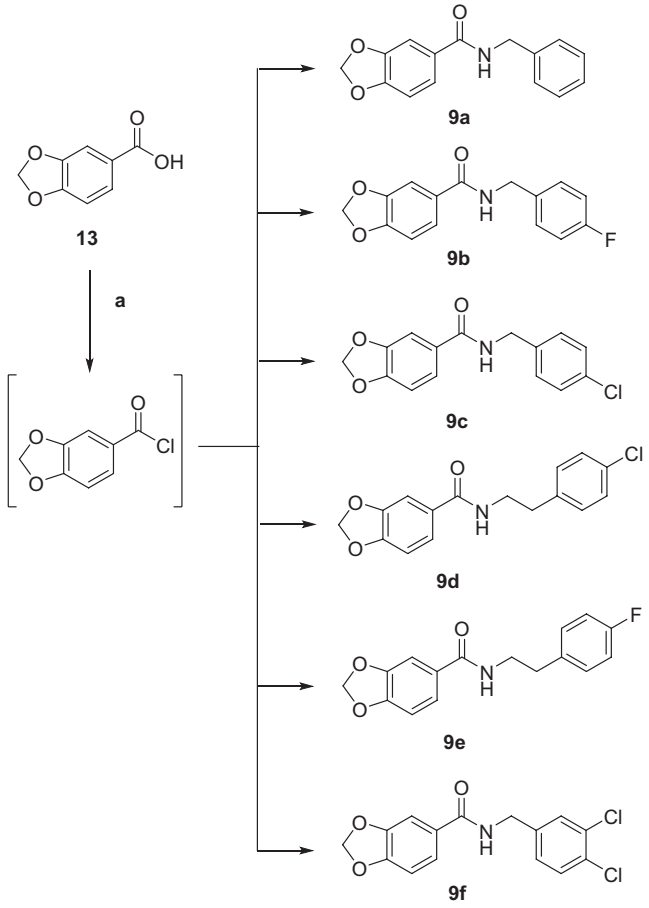

SCHEME 2 Synthesis of compounds **9a-f**. Piperonylic acid (1.00 eq.), $SOCl_2$ (2.00 eq.), DMF (0.01 eq.), $CHCl_3$ (10 mL), 25°C, 2 h; then, appropriate amine (1.50 eq.), TEA (2.00 eq.), dry DCM (15 mL), 25°C, 24 h.

antiproliferative activities, with the exception of compound **6f**, which bears a 3,4-dichlorobenzyl moiety. This compound reduced cell viability by almost 30% at 50 and 100 μM. The subset of compounds **7a-f**, which contain a 3,4-methylenedioxy cinnamic moiety as an acyl donor, displayed better efficacy in reducing cell viability than analogs **6a-f**. In fact, **7a-d** showed promising antiproliferative properties from 50 to 100 μM, with a degree of almost 40% at a 100 μM concentration. The most effective antiproliferative compounds resulted in **7e** and **7f**, bearing 4-fluorophenethyl and 3,4-dichlorobenzyl substituents, respectively. Sinapic acid was used to develop amides **8a-f**. This series of compounds showed different activities: **8a-b** seemed not useful in inducing cell death, while **8d-f** showed only a slight dose-dependent reduction in cell viability, with the strongest increase in cytotoxicity between 10 and 50 μM. Compound **8d**, bearing the 4-chlorobenzyl moiety, appeared to be the best antiproliferative compound of this subseries. Finally, compounds **9a-b** and **9d** failed to induce cell death, while **9e** showed very low activity at a concentration of 100 μM. On the other hand, **9c**, bearing the 4-chlorobenzyl moiety as **8c**, showed promising antiproliferative activity. The most interesting tool seemed **9f**, again with the 3,4-dichlorobenzyl substituent, showing an interesting antiproliferative activity (Figure 2). The highest cytotoxicity for compounds **7a**, **7e**, **7f**, **9c**, and **9f** was detected with IC_{50} values between 71 μM and 153 μM, calculated via GraphPad software (nonlinear regression) on the basis of the 5 different concentrations. In case of **7a** and **7e** the IC_{50} values are extrapolated as hypothetical values outside the curve. Normal intestinal epithelial cells (HCEC cell line) were less sensitive to these compounds (Figure 3), opening the way for further biological investigation in CRC cells.

2.2.2 | Compounds **7a**, **7e**, **7f**, **9c**, and **9f** induce cell cycle arrest and apoptosis

When performing a cell cycle analysis using PI staining and flow cytometry, we observed an increase in the G1 population after treating HCT116 tumor cells with **7a**, **7e**, **7f**, **9c**, and **9f** (Figure 4a,b), suggesting a stop in G1 phase. **9f** was the most effective, with a pre-G1 fraction of 17.4% (Figure 4a,b). These antiproliferative effects were verified by cell cycle FACS analysis with apoptotic cell fractions of 29.8% and 11.3% in HT29 and DLD1 cells, respectively, confirming the potential induction of apoptosis for this compound (Figure 4c,d). Nonmalignant HCEC cells did not respond to **9f** (Figure 4d). Compound **9f** was further tested in HT29 and DLD1 cells in a crystal violet assay, and IC_{50} values between 50 and 100 μM were found (Figure 5a). Next, we treated HCT116 cells with 99 μM **9f** for 48 h and analyzed different cell cycle proteins characteristic of the G1 phase by western blotting (Figure 5b). Both controls, untreated and DMSO-treated, were included. Corresponding to the FACS data, Cyclin D1 was decreased for the selected compounds, whereas the cell cycle inhibitor p21 showed a more variable profile. The highest levels were visible for **7a**, **7e**, and **9f** (Figure 5b). Again, **9f** showed the highest levels of cleaved poly (ADP-ribose) polymerase (PARP) signals, reflecting apoptosis induction (Figure 5b). To examine whether p21 induction was mediated by p53, the major upstream regulator of p21, we performed a western blot for p53 protein in HCT116 cells treated with **7a**, **7e**, **7f**, **9c**, and **9f** for 48 h. Only for **7a** and **9f**, we could detect similarly high levels of p21 and p53 (Figure 5b**)**. Next, we treated four other colon tumor cell lines, HT29, DLD1, SW480, and LoVo, with **9f** (99 μM, 48 h) and performed western blots for p21 and PARP. Indeed, p21 was upregulated in all cell lines, similar to apoptosis induction, which was detectable, with SW480 cells being the least responsive (Figure 5c). In contrast to the cell cycle analysis, normal HCEC cells also showed apoptosis induction visible as cleaved PARP bands (Figure 5c). The upregulation of p21 is in accordance with other studies showing that p21 could be involved in cell

17470285, 2024, 1, Downloaded from https://onlinelibrary.wiley.com/doi/10.1111/cbdd.14415 by CochraneItalia, Wiley Online Library on [17/01/2024]. See the Terms and Conditions (https://onlinelibrary.wiley.com/terms-and-conditions) on Wiley Online Library for rules of use; OA articles are governed by the applicable Creative Commons License

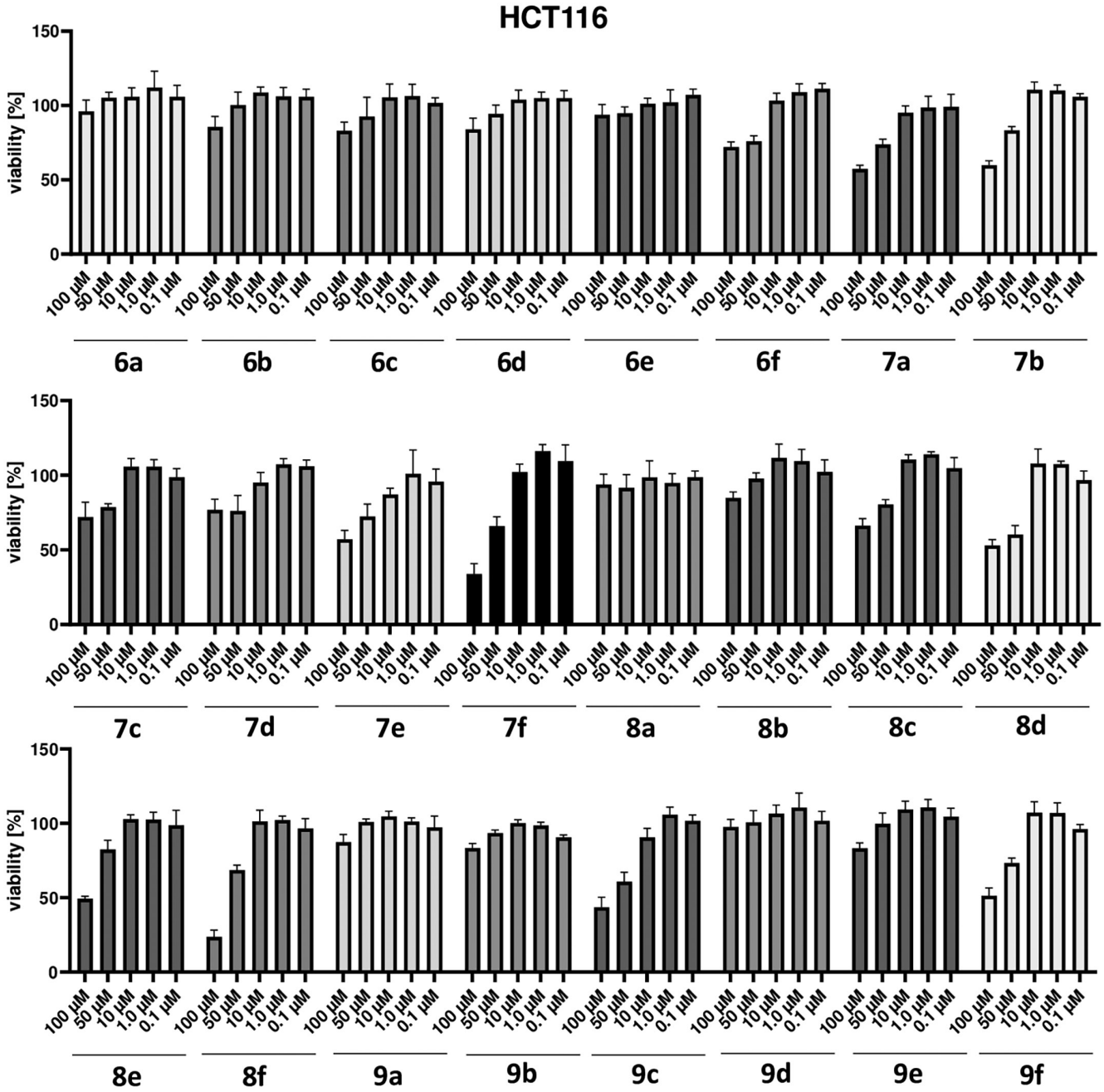

FIGURE 2 Compound screening for antitumor cytotoxicity. Crystal violet staining of HCT116 cells after treatment with compounds at various concentrations. HCT116 cells were treated for 48 h as described in the experimental section. Viability was normalized to DMSO-treated controls. Data represent the mean ±SD of two biological replicates with each three technical replicates.

cycle arrest and apoptosis induction (Ocker et al., 2019). Low Cyclin D1 levels confirmed the observed G1 arrest seen in the FACS analysis.

2.2.3 | Compounds **7a**, **7e**, **7f**, **9c**, and **9f** may affect the epigenetic machinery

One of the major regulatory mechanisms for the p21 gene is based on epigenetic control essentially mediated by histone deacetylase (HDAC) enzymes (Zupkovitz et al., 2010). Furthermore, HDAC inhibition strongly activates the expression of p21 (cip1/waf1) through enhanced histone acetylation around the p21 (cip1/waf1) promoter, and this expression is regulated in a p53-dependent and p53-independent manner (Ocker & Schneider-Stock, 2007). We treated HCT116 cells with our five compounds (**7a**, **7e**, **7f**, **9c**, **9f**) for 48 h and analyzed the expression of two histone deacetylases, HDAC1 and HDAC6, by western blotting. Interestingly, only HDAC1 levels were modestly decreased

17470285, 2024, 1, Downloaded from https://onlinelibrary.wiley.com/doi/10.1111/cbdd.14415 by CochraneItalia, Wiley Online Library on [17/01/2024]. See the Terms and Conditions (https://onlinelibrary.wiley.com/terms-and-conditions) on Wiley Online Library for rules of use; OA articles are governed by the applicable Creative Commons License

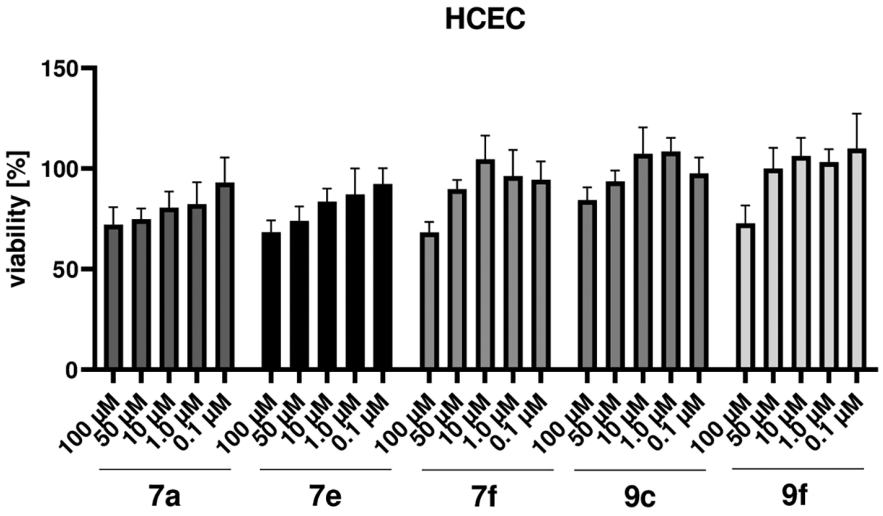

FIGURE 3 Compound screening for cytotoxicity against normal intestinal epithelial cells. Crystal violet staining of nontumor human colorectal epithelial HCECs after treatment with compounds at various concentrations. HCECs were treated for 48 h as described in the experimental section. Viability was normalized to DMSO-treated controls. Data represent the mean of two biological replicates with three technical replicates each.

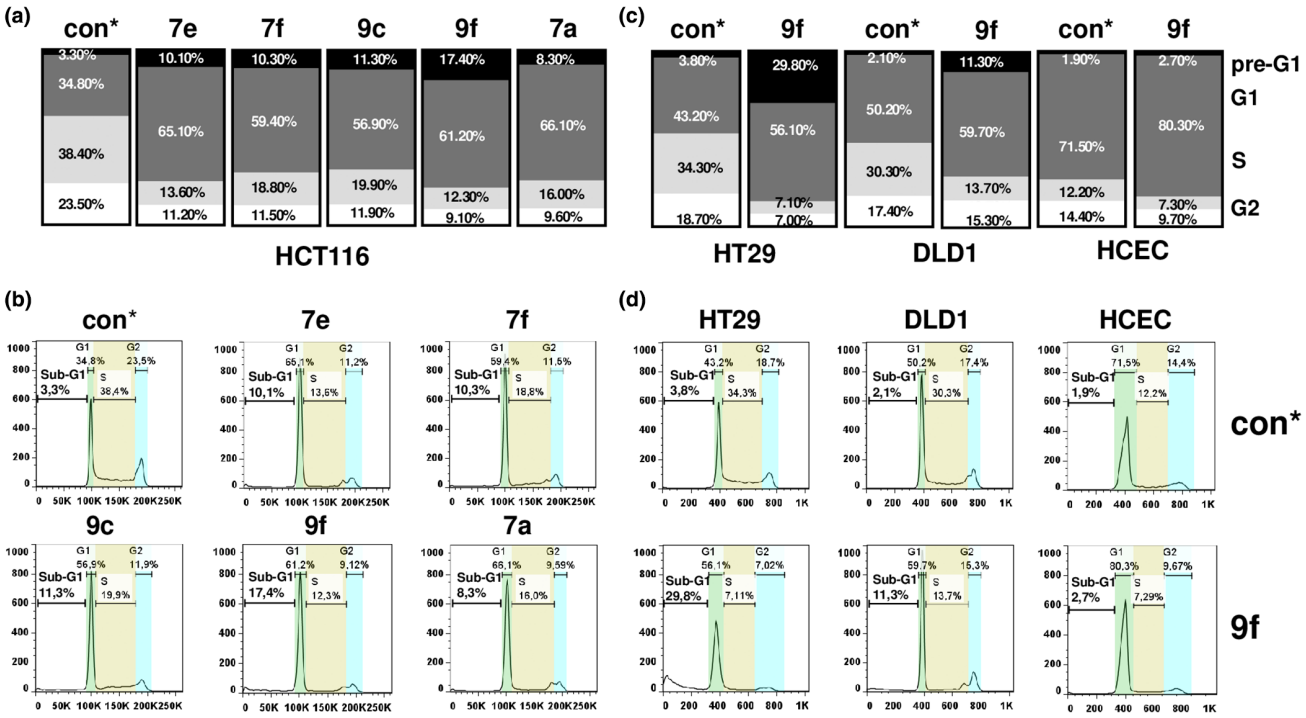

FIGURE 4 Compound effects on the cell cycle (a) Cell cycle analysis after 48 h treatment of HCT116 cells with IC_{50} concentrations (**7a**: 131 µM, **7e**: 153 µM, **7f**: 71 µM, **9c**: 76 µM, **9f**: 99 µM), stained with propidium iodide (PI) and analyzed by flow cytometry. Cells treated with DMSO served as controls. Treatment resulted in G1 arrest and an apoptotic pre-G1 population. The data shown are representative of two independent experiments. (b) Corresponding flow cytometry images for (a), (c) Cell cycle analysis after 48 h treatment of HT29 and DLD1 cells and nontumor human colorectal epithelial HCEC with 99 µM **9f**, stained with PI and analyzed by flow cytometry. Cells treated with DMSO served as controls. Treatment resulted in G1 arrest and an apoptotic pre-G1 population in the tumor cell lines but not in the nontumor cell line HCEC. The data shown are representative of two independent experiments. (d) Corresponding flow cytometry images for (c).

by compounds **9c** and **9f**, whereas HDAC6 levels were not affected (Figure S1a). Correspondingly higher levels of acetylated histone H3 (pan acH3) were visible for **9c** and **9f** but also for **7a** and **7e** (Figure S1a). Next, we treated four other colon tumor cells and the nonmalignant colon epithelial cell line HCEC with **9f** (99 µM, 48 h) and examined the HDAC1

17470285, 2024, 1, Downloaded from https://onlinelibrary.wiley.com/doi/10.1111/cbdd.14415 by CochraneItalia, Wiley Online Library on [17/01/2024]. See the Terms and Conditions (https://onlinelibrary.wiley.com/terms-and-conditions) on Wiley Online Library for rules of use; OA articles are governed by the applicable Creative Commons License

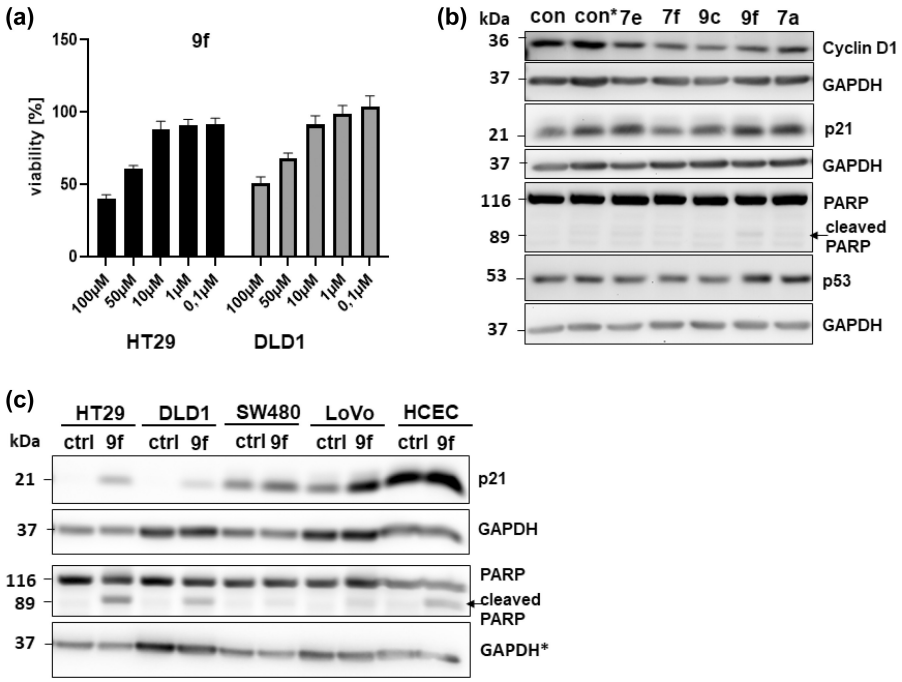

FIGURE 5 Anticancer compound effects on viability and cell cycle-mediating proteins (a) Crystal violet staining of HT29 and DLD1 cells after 48 h treatment with **9f** at various concentrations. Viability was normalized to DMSO-treated controls. Data represent the mean ± SD of two biological replicates with each three technical replicates. (b) Western blot analysis of HCT116 cells after 48 h treatment with IC_{50} concentrations (**7a**: 131 µM, **7e**: 153 µM, **7f**: 71 µM, **9c**: 76 µM, **9f**: 99 µM) and analysis by western blotting. Untreated cells (con) or DMSO-treated cells (con*) served as controls. The data shown are representative of two independent experiments. (c) Western blot analysis of different colorectal cancer cell lines and the nontumor cell line HCEC after 48 h treatment with **9f** (99 µM). Cells treated with DMSO served as controls. The data shown are representative of two independent experiments. *The GAPDH bands are also shown in Figure S1b for HDAC1 and pan-acH3 as the markers were detected on the same membrane.

and pan acH3 levels by western blotting. We confirmed a general and very modest decreasing effect on HDAC1, except in DLD1 cells (Figure S1b). An increase in pan acH3 levels was observed for HT29, DLD1, and SW480 cells but not for LoVo cells. We have already reported that a decrease in HDAC1 levels by HDAC inhibitor treatment is accompanied by activation of p21, mainly caused by increased acetylation of histones around the p21 promoter (Ocker et al., 2019; Ocker & Schneider-Stock, 2007). Here, **9f** induced cell cycle arrest in G1 phase and showed pro-apoptotic effects in flow cytometry and western blot (Figures 4a–d and 5a–c). Of note, HT29 cells with a mutant p53 and serine/threonine-protein kinase B-Raf (BRAF) are highly resistant to diverse chemotherapeutic drugs (El Khoury et al., 2016), but compound **9f** seemed to have the potential to overcome the resistance mechanisms of HT29 cells (Figures 4c,d and 5a,c).

3 | METHODS

3.1 | General chemistry methods

Carboxylic acids and amines were purchased from Merck (Milan, Italy) and used without further purification. All reactions were performed under a nitrogen atmosphere using oven-dried glassware and anhydrous solvents. Flash column chromatography was carried out on silica gel (Merck: Kieselgel 60, particle size 0.040–0.063 mm). Reactions were monitored by thin-layer chromatography (TLC), carried out using glass-backed plates coated with Merck Kieselgel 60 GF254. Plates were visualized under UV light (at 254 nm). ^{1}H NMR and ^{13}C NMR spectra were recorded on a Varian 300 MHz spectrometer using the residual signal of the deuterated solvent as an internal standard. Coupling constants (*J*) are given in hertz (Hz). Splitting patterns are described as singlet (s), doublet (d), triplet (t), quartet (q), and broad (brs); the values of chemical shifts (δ) are given in parts per million (ppm). ESI-HRMS spectra were acquired by a linear ion-trap-Orbitrap hybrid mass spectrometer (LTQOrbitrap XL) (Thermo Fisher Scientific, Bremen, Germany) operating in positive electrospray ionization mode. Data were collected and analyzed using the Xcalibur 2.2 software provided by the manufacturer. Yields refer to purified products and are not optimized. The purity of the final products (>95%) was determined by an analytical HPLC Merk Purospher STAR RP-18e (5 µm) LiChroCART 250–4 column; detection at 254 nm;

17470285, 2024, 1, Downloaded from https://onlinelibrary.wiley.com/doi/10.1111/cbdd.14415 by CochraneItalia, Wiley Online Library on [17/01/2024]. See the Terms and Conditions (https://onlinelibrary.wiley.com/terms-and-conditions) on Wiley Online Library for rules of use; OA articles are governed by the applicable Creative Commons License

flow rate = 1.0 mL/min; mobile phase A, 0.01% trifluoroacetic acid (TFA) (v/v) in water; mobile B, acetonitrile; gradient, 90/10–10/90 A/B in 20 min. The gradient was optimized based on compound polarity.

3.2 | General procedure for the synthesis of compounds 6a-f, 7a-f, and 8a-f

To a well-stirred solution of acids **10**–**12** (1.00 eq.) in dry DMF (10 mL), the appropriate amine (1.20 eq.), EDCI (2.10 eq.), and HOBt (1.50 eq.) were added. The mixture was stirred at 25°C for 24 h. After that, the mixture was treated with a saturated aqueous solution of $NaHCO_3$ and extracted with EtOAc (1 × 20 mL). The organic layer was then treated with a saturated solution of NH_4Cl (2 × 15 mL). The combined organics were dried (Na_2SO_4), filtered, and evaporated under reduced pressure. The residue was purified through flash column chromatography on silica gel (eluent PE/EtOAc, 3:1 for **6a-f**, PE/EtOAc 4:1 for **7a-f** or PE/EtOAc 1:1 for **8a-f**).

3.3 | General procedure for the synthesis of compounds 9a-f

To a well-stirred solution of piperonilic acid **13** (100 mg, 0.78 mmol, 1.00 eq.) in chloroform (10 mL), thionyl chloride (114 μL, 1.56 mmol, 2.00 eq.) and DMF (cat.) were added. The mixture was stirred for 2 h at 25°C; then, the chloroform was removed, and the crude material was diluted in dry dichloromethane (DCM) (20 mL). The appropriate amine (1.5 eq.) and triethylamine (217 μL, 1.56 mmol, 2.00 eq.) were added, and the mixture was stirred at 25°C for 24 h. Then, the solvent was removed, and the crude solution was diluted with EtOAc extracted with NH_4Cl (3 × 10 mL). The organic layer was dried (Na_2SO_4), filtered, and evaporated under reduced pressure. The residue was purified through flash column chromatography on silica gel (eluent PE/EtOAc, 1:1).

3.4 | Biological methods

3.4.1 | Cell culture

Colon carcinoma cell lines HCT116, HT29, DLD1, SW480, and LoVo were cultured in 10 cm cell culture dishes (Corning) in RPMI (PAN) supplemented with 10% fetal bovine serum (PAN) and penicillin (100 U/mL)/streptomycin (100 mg/mL) (PAN) at 37°C and 5% CO_2 in a humidified atmosphere. HCEC cells were maintained in 10 cm CellBIND® dishes (Corning) in basal HCEC medium (PAN) supplemented with 2 mM L-glutamine (GlutaMax®, Gibco), 30 μg/mL bovine pituitary extract (PromoCell), 38 μg/mL ascorbic acid (Sigma Aldrich), 1 nM dexamethasone (Sigma Aldrich), and 100 mM retinol (Sigma Aldrich) at 37°C and 5% CO_2 in a humidified atmosphere. Cells were passaged every 3–4 days. Cell line verification was performed through Multiplex Cell Authentication by Multiplexing (Heidelberg, Germany). The mycoplasma-free status of the cells was verified.

3.4.2 | Crystal violet assay

Crystal violet assays were conducted as previously described (Carullo, Mazzotta, et al., 2020) to test the substances for their effects on cell viability. For this, 7500 cells were plated in 100 μL of cell culture medium per well of a 96-well plate (Corning) and allowed to settle for 24 h at 37°C and 5% CO_2. Then, the cells were treated with the test substances at the stated concentrations for 48 h. Afterward, the cells were stained with crystal violet for 15 min at room temperature. The absorbance at 595 nm was measured by a Victor® X3 (Perkin Elmer). The IC_{50} concentration was calculated via GraphPad software (nonlinear regression).

3.4.3 | Western blot analysis

To determine alterations in protein levels, western blot analysis was performed as described previously. To treat the cells, 0.55×10^5 cells were seeded in 6 cm cell culture dishes (Corning) and allowed to adhere at 37°C and 5% CO_2 for 24 h. The cells were then treated with the substances (**7a**: 131 μM, **7e**: 153 μM, **7f**: 71 μM, **9c**: 76 μM, **9f**: 99 μM) and incubated at 37°C with 5% CO_2 for 48 h. For Western blot analysis, 40 μg of total protein was run in 12%, 10%, or 7.5% denaturing SDS–PAGE and transferred onto 0.2 μm nitrocellulose membranes overnight. Unspecific binding sites were blocked with 5% milk powder in TBS-T buffer for 1 h at RT. Incubation with primary antibodies was performed overnight at 4°C: anti-CyclinD1-IgG (1:1.000, Cell Signaling, #2922), anti-p21-IgG (1:5.000, Cell Signaling, #2947), anti-PARP-IgG (1:2.000, Cell Signaling, #9532), anti-p53-IgG-HRP (1:1.000, Santa Cruz, #sc-126-HRP), anti-HDAC1-IgG (1:1.000, Active Motif, #39531), anti-HDAC6-IgG (1:15.000, Cell Signaling, #7558), or anti-acH3-IgG (1:15.000, Active Motif, #39040). Then, the blots were incubated with secondary HRP-coupled antibodies goat-anti-mouse IgG (H + L) (1:10.000, Thermo Fisher Scientific, #A-11029) or goat-anti-rabbit IgG (H + L) (1:10.000, Thermo Fisher Scientific, #31460) for 1 h at RT. GAPDH was used to control equal loading of the

17470285, 2024, 1, Downloaded from https://onlinelibrary.wiley.com/doi/10.1111/cbdd.14415 by CochraneItalia, Wiley Online Library on [17/01/2024]. See the Terms and Conditions (https://onlinelibrary.wiley.com/terms-and-conditions) on Wiley Online Library for rules of use; OA articles are governed by the applicable Creative Commons License

samples. The blots were incubated with HRP-labelled anti-GAPDH-IgG1 (1:100.000, Abnova, #MAB5476) for 45 min at RT. The blots were developed with the Immobilon Western Chemiluminescent horseradish peroxidase (HRP) substrate kit (Merck Millipore). Photographs were taken using a GeneGnome (Syngene).

3.4.4 | Cell cycle analysis

Cell cycle analysis by staining of DNA with propidium iodide (PI) and detection using flow cytometry was performed as previously described (Carullo, Mazzotta, et al., 2020; Parupalli et al., 2023). A total of 5.5×10^5 cells (HCT116, HT29, DLD1, SW480, LoVo) or 4×10^5 cells (HCEC) were plated in 6 cm cell culture dishes (Corning) and then left to adhere at 37°C and 5% CO_2 for 24 h. Then, the cells were treated with the substances (**7a**: 131 μM, **7e**: 153 μM, **7f**: 71 μM, **9c**: 76 μM, **9f**: 99 μM) for 48 h. Floating and adherent cells were harvested by trypsinization. Afterwards, the cells were centrifuged, washed with PBS, and fixed in 70% ice-cold ethanol overnight at 4°C. The DNA was stained with a staining solution containing 150 μg/mL PI and 0.5 mg/mL RNase for 30 min at RT in the dark. The DNA content of the cells was measured with a fluorescent activated cell sorter (FACS) FACSCanto II (BD Biosciences), and the cell cycle distribution was identified using FlowJo software (v7.6.5, FlowJo LCC).

4 | CONCLUSION

Based on the structures of natural compounds such as cinnamic acids and piperonilic acid, we synthesized amides **6-9a-f**, with the aim of obtaining new molecular entities for the treatment of CRC. In particular, amides were developed as versatile tools in anticancer research. The developed compounds **6-9a-f** were first assayed in the HCT116 cell line by means of a crystal violet assay, showing modest antiproliferative properties that were further confirmed in HT29, LoVo, and SW480 cells, without eliciting significant toxic effects in normal HCEC cells. In this context, the cell cycle analyses revealed the induction of apoptosis as the preferred cell death mechanism. The cleavage of PARP and the modulation of the p53/p21 axis are signs of DNA interference in cancer cells. In conclusion, the reported experimental data provided preliminary data highlighting that several synthesized compounds based on natural scaffolds of cinnamic acids have the potential to behave as lead compounds with apoptosis-inducing effects, but further studies are needed for rational drug design of new antiproliferative agents targeting the p21/HDAC mediated epigenetic machinery.

ACKNOWLEDGEMENTS

Not applicable.

FUNDING INFORMATION

Not applicable.

DATA AVAILABILITY STATEMENT

The data that support the findings of this study are available on request from the corresponding author. The data are not publicly available due to privacy or ethical restrictions.

ORCID

Sandra Gemma https://orcid.org/0000-0002-8313-2417
Adrian Koch https://orcid.org/0000-0001-5387-4906
Sarah Mazzotta https://orcid.org/0000-0003-0029-7003
Gabriele Carullo https://orcid.org/0000-0002-1619-3295
Anna Ramunno https://orcid.org/0000-0003-1089-2439
Stefania Butini https://orcid.org/0000-0002-8471-0880
Regine Schneider-Stock https://orcid.org/0000-0003-0482-531X
Giuseppe Campiani https://orcid.org/0000-0001-5295-9529
Francesca Aiello https://orcid.org/0000-0001-6846-5582

REFERENCES

Carullo, G., Ahmed, A., Trezza, A., Spiga, O., Brizzi, A., Saponara, S., Fusi, F., & Aiello, F. (2020). Design, synthesis and pharmacological evaluation of ester-based quercetin derivatives as selective vascular KCa1.1 channel stimulators. *Bioorganic Chemistry*, *105*, 104404.

Carullo, G., Ahmed, A., Trezza, A., Spiga, O., Brizzi, A., Saponara, S., Fusi, F., & Aiello, F. (2021). A multitarget semi-synthetic derivative of the flavonoid morin with improved in vitro vasorelaxant activity: Role of CaV1.2 and KCa1.1 channels. *Biochemical Pharmacology*, *185*, 114429.

Carullo, G., Falbo, F., Ahmed, A., Trezza, A., Gianibbi, B., Nicolotti, O., Campiani, G., Aiello, F., Saponara, S., & Fusi, F. (2023). Artificial intelligence-driven identification of morin analogues acting as CaV1.2 channel blockers: Synthesis and biological evaluation. *Bioorganic Chemistry*, *131*, 106326.

Carullo, G., Governa, P., Leo, A., Gallelli, L., Citraro, R., Cione, E., Caroleo, M. C., Biagi, M., Aiello, F., & Manetti, F. (2019). Quercetin-3-Oleate contributes to skin wound healing targeting FFA1/GPR40. *ChemistrySelect*, *4*, 8429–8433.

Carullo, G., Mazzotta, S., Koch, A., Hartmann, K. M., Friedrich, O., Gilbert, D. F., Vega-Holm, M., Schneider-Stock, R., & Aiello, F. (2020). New Oleoyl hybrids of natural antioxidants: Synthesis and in vitro evaluation as inducers of apoptosis in colorectal cancer cells. *Antioxidants*, *9*(11), 1077.

Carullo, G., Perri, M., Manetti, F., Aiello, F., Caroleo, M. C., & Cione, E. (2019). Quercetin-3-oleoyl derivatives as new GPR40 agonists: Molecular docking studies and functional evaluation. *Bioorganic & Medicinal Chemistry Letters*, *29*, 1761–1764.

17470285, 2024, 1, Downloaded from https://onlinelibrary.wiley.com/doi/10.1111/cbdd.14415 by CochraneItalia, Wiley Online Library on [17/01/2024]. See the Terms and Conditions (https://onlinelibrary.wiley.com/terms-and-conditions) on Wiley Online Library for rules of use; OA articles are governed by the applicable Creative Commons License

Carullo, G., Saponara, S., Ahmed, A., Gorelli, B., Mazzotta, S., Trezza, A., Gianibbi, B., Campiani, G., Fusi, F., & Aiello, F. (2022). Novel Labdane Diterpenes-based synthetic derivatives: Identification of a Bifunctional vasodilator that inhibits CaV1.2 and stimulates KCa1.1 channels. *Marine Drugs*, *20*, 515.

Darakhshan, S., & Pour, A. B. (2015). Tranilast: A review of its therapeutic applications. *Pharmacological Research*, *91*, 15–28.

El Khoury, F., Corcos, L., Durand, S., Simon, B., & Le Jossic-Corcos, C. (2016). Acquisition of anticancer drug resistance is partially associated with cancer stemness in human colon cancer cells. *International Journal of Oncology*, *49*, 2558–2568.

Ertl, P., Altmann, E., & Mckenna, J. M. (2020). The Most common functional groups in bioactive molecules and how their popularity has evolved over time. *Journal of Medicinal Chemistry*, *63*, 8408–8418.

Federico, S., Khan, T., Fontana, A., Brogi, S., Benedetti, R., Sarno, F., Carullo, G., Pezzotta, A., Saraswati, A. P., Passaro, E., Pozzetti, L., Papa, A., Relitti, N., Gemma, S., Butini, S., Pistocchi, A., Ramunno, A., Vincenzi, F., Varani, K., … Campiani, G. (2022). Azetidin-2-one-based small molecules as dual hHDAC6/HDAC8 inhibitors: Investigation of their mechanism of action and impact of dual inhibition profile on cell viability. *European Journal of Medicinal Chemistry*, *238*, 114409.

Garmpis, N., Damaskos, C., Garmpi, A., Nonni, A., Georgakopoulou, V. E., Antoniou, E., Schizas, D., Sarantis, P., Patsouras, A., Syllaios, A., Vallilas, C., Koustas, E., Kontzoglou, K., Trakas, N., & Dimitroulis, D. (2021). Histone deacetylases and their inhibitors in colorectal cancer therapy: Current evidence and future considerations. *Current Medicinal Chemistry*, *29*, 2979–2994.

Ghosh, A. K., & Shahabi, D. (2021). Synthesis of amide derivatives for electron deficient amines and functionalized carboxylic acids using EDC and DMAP and a catalytic amount of HOBt as the coupling reagents. *Tetrahedron Letters*, *63*, 152719.

Hazafa, A., Iqbal, M. O., Javaid, U., Tareen, M. B. K., Amna, D., Ramzan, A., Piracha, S., & Naeem, M. (2022). Inhibitory effect of polyphenols (phenolic acids, lignans, and stilbenes) on cancer by regulating signal transduction pathways: A review. *Clinical and Translational Oncology*, *24*, 432–445.

Heleno, S. A., Martins, A., Queiroz, M. J. R. P., & Ferreira, I. C. F. R. (2015). Bioactivity of phenolic acids: Metabolites versus parent compounds: A review. *Food Chemistry*, *173*, 501–513.

Kobzar, O. L., Tatarchuk, A. V., Mrug, G. P., Bondarenko, S. P., Demydchuk, B. A., Frasinyuk, M. S., & Vovk, A. I. (2023). Carboxylated chalcones and related flavonoids as inhibitors of xanthine oxidase. *Medicinal Chemistry Research*, *8*, 1804–1815.

Lee, H. Y., Tang, D. W., Liu, C. Y., & Cho, E. C. (2022). A novel HDAC1/2 inhibitor suppresses colorectal cancer through apoptosis induction and cell cycle regulation. *Chemico-Biological Interactions*, *352*, 109778.

Mazzotta, S., Carullo, G., Sciubba, F., Di Cocco, M. E., & Aiello, F. (2021). 7-Docosahexaenoyl-Quercetin. *Molbank*, *2021*, M1203.

Natella, F., Nardini, M., Di Felice, M., & Scaccini, C. (1999). Benzoic and Cinnamic acid derivatives as antioxidants: Structure–activity relation. *Journal of Agricultural and Food Chemistry*, *47*, 1453–1459.

Nazir, Y., Rafique, H., Roshan, S., Shamas, S., Ashraf, Z., Rafiq, M., Tahir, T., Qureshi, Z. U. R., Aslam, A., & Asad, M. H. H. B. (2022). Molecular docking, synthesis, and Tyrosinase inhibition activity of Acetophenone amide: Potential inhibitor of Melanogenesis. *BioMed Research International*, 1040693.

Nazir, Y., Saeed, A., Rafiq, M., Afzal, S., Ali, A., Latif, M., Zuegg, J., Hussein, W. M., Fercher, C., Barnard, R. T., Cooper, M. A., Blaskovich, M. A. T., Ashraf, Z., & Ziora, Z. M. (2020). Hydroxyl substituted benzoic acid/cinnamic acid derivatives: Tyrosinase inhibitory kinetics, anti-melanogenic activity and molecular docking studies. *Bioorganic & Medicinal Chemistry Letters*, *30*, 126722.

Ocker, M., Al Bitar, S., Monteiro, A. C., Gali-Muhtasib, H., & Schneider-Stock, R. (2019). Epigenetic regulation of p21cip1/waf1 in human cancer. *Cancers*, *11*, 1343.

Ocker, M., & Schneider-Stock, R. (2007). Histone deacetylase inhibitors: Signalling towards p21cip1/waf1. *The International Journal of Biochemistry & Cell Biology*, *39*, 1367–1374.

Parupalli, R., Akunuri, R., Spandana, A., Phanindranath, R., Pyreddy, S., Bazaz, M. R., Vadakattu, M., Joshi, S. V., Bujji, S., Gorre, B., Yaddanapudi, V. M., Dandekar, M. P., Reddy, V. G., Nagesh, N., & Nanduri, S. (2023). Synthesis and biological evaluation of 1-phenyl-4,6-dihydrobenzo[b]pyrazolo[3,4-d]azepin-5(1H)-one/thiones as anticancer agents. *Bioorganic Chemistry*, *135*, 106478.

Pozzetti, L., Ibba, R., Rossi, S., Taglialatela-Scafati, O., Taramelli, D., Basilico, N., D'Alessandro, S., Parapini, S., Butini, S., Campiani, G., & Gemma, S. (2022). Total synthesis of the natural Chalcone Lophirone E, synthetic studies toward Benzofuran and indole-based analogues, and investigation of anti-Leishmanial activity. *Molecules*, *27*, 463.

Relitti, N., Saraswati, A. P., Chemi, G., Brindisi, M., Brogi, S., Herp, D., Schmidtkunz, K., Saccoccia, F., Ruberti, G., Ulivieri, C., & Vanni, F. (2020). Novel quinolone-based potent and selective HDAC6 inhibitors: Synthesis, molecular modeling studies and biological investigation. *European Journal of Medicinal Chemistry*, *90*, 112998.

Saraswati, A. P., Relitti, N., Brindisi, M., Osko, J. D., Chemi, G., Federico, S., Grillo, A., Brogi, S., McCabe, N. H., Turkington, R. C., Ibrahim, O., O'Sullivan, J., Lamponi, S., Ghanim, M., Kelly, V. P., Zisterer, D., Amet, R., Hannon Barroeta, P., Vanni, F., … Campiani, G. (2020). Spiroindoline-capped selective HDAC6 inhibitors: Design, synthesis, structural analysis, and biological evaluation. *ACS Medicinal Chemistry Letters*, *11*, 2268–2276.

Sirous, H., Campiani, G., Calderone, V., & Brogi, S. (2021). Discovery of novel hit compounds as potential HDAC1 inhibitors: The case of ligand- and structure-based virtual screening. *Computers in Biology and Medicine*, *137*, 104808.

Spizzirri, U. G., Carullo, G., De Cicco, L., Crispini, A., Scarpelli, F., Restuccia, D., & Aiello, F. (2019). Synthesis and characterization of a (+)-catechin and L-(+)-ascorbic acid cocrystal as a new functional ingredient for tea drinks. *Heliyon*, *5*, e02291.

Vaishnav, A., Ogre, P., & Vaishnav, M. A. (2023). Chalcones as next-generation antimicrobial agents: Deep insights into anti-infective perspectives and novel synthesis routes. *International journal of Medical & Pharmaceutical Sciences*, *13*(7), 1–6.

Xu, Z., Lu, S., Liu, X., Tang, L., Liu, Z., Cui, J., Wang, W., Lu, W., & Huang, J. (2023). Drug repurposing of ilepcimide that ameliorates experimental autoimmune encephalomyelitis via restricting inflammatory response and oxidative stress. *Toxicology and Applied Pharmacology*, *458*, 116328.

Zahrani, N. A. A. L., El-Shishtawy, R. M., & Asiri, A. M. (2020). Recent developments of gallic acid derivatives and their hybrids in medicinal chemistry: A review. *European Journal of Medicinal Chemistry*, *204*, 112609.

Zhao, Z., Song, H., Xie, J., Liu, T., Zhao, X., Chen, X., He, X., Wu, S., Zhang, Y., & Zheng, X. (2019). Research progress in the biological activities of 3,4,5-trimethoxycinnamic acid (TMCA) derivatives. *European Journal of Medicinal Chemistry*, *173*, 213–227.

17470285, 2024, 1, Downloaded from https://onlinelibrary.wiley.com/doi/10.1111/cbdd.14415 by CochraneItalia, Wiley Online Library on [17/01/2024]. See the Terms and Conditions (https://onlinelibrary.wiley.com/terms-and-conditions) on Wiley Online Library for rules of use; OA articles are governed by the applicable Creative Commons License

Zupkovitz, G., Grausenburger, R., Brunmeir, R., Senese, S., Tischler, J., Jurkin, J., Rembold, M., Meunier, D., Egger, G., Lagger, S., Chiocca, S., Propst, F., Weitzer, G., & Seiser, C. (2010). The cyclin-dependent kinase inhibitor p21 is a crucial target for histone deacetylase 1 as a regulator of cellular proliferation. *Molecular and Cellular Biology*, *30*, 1171–1181.

SUPPORTING INFORMATION

Additional supporting information can be found online in the Supporting Information section at the end of this article.

How to cite this article: Falbo, F., Gemma, S., Koch, A., Mazzotta, S., Carullo, G., Ramunno, A., Butini, S., Schneider-Stock, R., Campiani, G., & Aiello, F. (2023). Synthetic derivatives of natural cinnamic acids as potential anti-colorectal cancer agents. *Chemical Biology & Drug Design*, *103*, e14415. https://doi.org/10.1111/cbdd.14415

17470285, 2024, 1, Downloaded from https://onlinelibrary.wiley.com/doi/10.1111/cbdd.14415 by CochraneItalia, Wiley Online Library on [17/01/2024]. See the Terms and Conditions (https://onlinelibrary.wiley.com/terms-and-conditions) on Wiley Online Library for rules of use; OA articles are governed by the applicable Creative Commons License